Short Communication

Establishment of an Improved Mouse Model for Infantile Neuroaxonal Dystrophy That Shows Early Disease Onset and Bears a Point Mutation in *Pla2g6*

Haruka Wada,* Takuwa Yasuda,† Ikuo Miura,‡
Kazuhiko Watabe,§ Chika Sawa,*¶
Hajime Kamijuku,* Satoshi Kojo,*
Masaru Taniguchi,‖ Ichizo Nishino,**
Shigeharu Wakana,‡ Hisahiro Yoshida,†
and Ken-ichiro Seino*

From the Division of Bioregulation Research,* Institute of Medical Science, St. Marianna University School of Medicine, Kanagawa; the Laboratories for Immunogenetics‡ and Immune Regulation,‖ RIKEN Research Center for Allergy and Immunology, RIKEN Yokohama Institute, Kanagawa; the Technology and Development Team for Mouse Genotype Analysis,‡ Japan Mouse Clinic RIKEN Bio-resource Center, Ibaraki; the Department of Molecular Neuropathology,§ Tokyo Metropolitan Institute for Neuroscience, Tokyo; the Molecular Pharmacology,¶ Argenes, Inc., Tokyo; and the Department of Neuromuscular Research,** National Institute of Neuroscience, Tokyo, Japan

Calcium-independent group VIA phospholipase A₂ (iPLA₂β), encoded by *PLA2G6*, has been shown to be involved in various physiological and pathological processes, including immunity, cell death, and cell membrane homeostasis. Mutations in the *PLA2G6* gene have been recently identified in patients with infantile neuroaxonal dystrophy (INAD). Subsequently, it was reported that similar neurological impairment occurs in gene-targeted mice with a null mutation of iPLA₂β, whose disease onset became apparent approximately 1 to 2 years after birth. Here, we report the establishment of an improved mouse model for INAD that bears a point mutation in the ankyrin repeat domain of *Pla2g6* generated by *N*-ethyl-*N*-nitrosourea mutagenesis. These mutant mice developed severe motor dysfunction, including abnormal gait and poor performance in the hanging grip test, as early as 7 to 8 weeks of age, in a manner following Mendelian law. Neuropathological examination revealed widespread formation of spheroids containing tubulovesicular membranes similar to human INAD. Molecular and biochemical analysis revealed that the mutant mice expressed Pla2g6 mRNA and protein, but the mutated Pla2g6 protein had no glycerophospholipid-catalyzing enzyme activity. Because of the significantly early onset of the disease, this mouse mutant (*Pla2g6-inad*) could be highly useful for further studies of pathogenesis and experimental interventions in INAD and neurodegeneration. *(Am J Pathol 2009, 175:2257–2263; DOI: 10.2353/ajpath.2009.090343)*

Phospholipases A₂ (PLA₂) are a diverse group of enzymes that catalyze the hydrolysis of *sn*-2 fatty acid substituents to yield a free fatty acid and a 2-lysophospholipid. PLA₂s are classified into various groups on the basis of Ca^{2+} requirement and sequence homology. These include secretory PLA₂s, the group IV cytosolic PLA₂s, and the group VI Ca^{2+}-independent (i) PLA₂s.[1] The group VIA iPLA₂, designated iPLA₂β and encoded by the *PLA2G6* gene, is an 85- to 88-kDa cytosolic PLA₂ whose amino acid sequence includes eight N-terminal ankyrin repeats, a caspase-3 cleavage site, an ATP-binding domain, a serine lipase consensus sequence (GXSXG), a bipartite nuclear localization sequence, and a C-terminal calmodulin-binding domain.[2] iPLA₂β does not require Ca^{2+} for its catalytic activity and is suggested to play important roles in remodeling of membrane phospholipids, signal transduction, cell proliferation, and apoptosis.[2]

Recently, it has been shown that a genetic defect in *PLA2G6* leads to a human disease. In fact, mutations in the *PLA2G6* gene were identified in patients with a rare neurodegenerative disorder of humans, infantile neuro-axonal dystrophy (INAD).[3,4] INAD usually begins within the first few years of life and leads to progressive impairment of movement and cognition. The pathological hallmark of the disease is the presence of large spheroids containing accumulated material primarily located in distal axons and nerve terminals.[5,6] These pathological changes are widely distributed throughout the brain and are also often found in peripheral nerves. A common feature of spheroids characterized by electron microscopy studies is the accumulation of membranes with tubulovesicular structures.[7]

Morgan et al[3] identified a total of 44 unique *PLA2G6* mutations in patients with INAD. Mutations were present in both alleles in all but one patient. In a few patients, there were early frameshift and stop codon mutations, which seemed to cause a complete loss of $iPLA_2\beta$ protein and function. However, the rest (32 patients) had missense mutations distributed throughout the gene ,causing single amino acid substitutions. Several patients had the mutation in the serine lipase consensus sequence (GXSXG), but most of the patients had the mutation in various regions independent from the lipase domain. Therefore, the precise mechanism of how mutation of *PLA2G6* causes the neurodegenerative disease is obscure.

N-Ethyl-*N*-nitrosourea (ENU) is a mutagen that randomly induces point mutations throughout the genome. ENU mutagenesis has been widely used for generating mouse mutants.[8] In a standard ENU mutagenesis regimen, we have found a mouse mutant that showed a gross appearance of motor dysfunction developing as early as 7 to 8 weeks of age in a recessive inherited manner. Using an outcross backcross breeding scheme and subsequent chromosomal mapping, we identified the chromosomal location of the affected region. Sequencing a candidate gene in the mutant mouse allowed us to identify the causative mutation as a point mutation in the ankyrin repeat of *Pla2g6* causing an amino acid substitution. Biochemical analysis of the mutated Pla2g6 protein showed that the point mutation in the ankyrin repeat leads to a compete loss of enzyme activity of Pla2g6. Because of the early onset of the disease induced by the point mutation, which is often observed in most of patients with INAD, this mouse mutant seems exceedingly useful to elucidate the mechanism of neurodegeneration underlying INAD and to study a novel therapeutic strategy for neurodegenerative disease including INAD and Parkinson's disease.

Materials and Methods

ENU Mutagenesis, Breeding of Mice, and Screening for Mouse Mutants

ENU mutagenesis was performed as described previously.[9] In brief, we injected ENU (Sigma-Aldrich, Japan, Tokyo) i.p. into C57BL/6J Jcl (B6) male mice (Japan CLEA, Tokyo, Japan) at 8 to 10 weeks of age with body weight of 85 mg/kg. The injections were performed twice at weekly intervals. The injected male mice were mated with wild-type B6 female mice by an in vitro fertilization-embryo transfer procedure after a sterile period (approximately 10 to 11 weeks) to produce the first generation (G1) offspring. The G1 male mice were mated again with wild-type B6 female mice to obtain the second generation (G2) harboring the ENU mutation at a 50% ratio of the first generation. The third generation (G3) was made by G2 sib-mating. Every reproduction step was done by in vitro fertilization-embryo transfer to obtain a large number of offspring at the same developmental stage. Because the estimated incidence of homozygote offspring in G3 was 1 of 16, more than 48 mice were produced in a pedigree at the same birthday. We screened approximately 100 G3 mice every week with a comprehensive set of phenotype assays including behavioral tests, blood tests, and measurement of locomotor activity in their home cages.[9]

### Chromosomal Mapping and Sequencing of the Candidate Gene

Chromosomal mapping was based on an outcross of homozygous mutant mice (B6) to C3H (Japan CLEA) followed by a subsequent brother-sister mating.[9] A genome-wide microsatellite marker panel was applied to pooled tail DNA from 51 mutant mice to determine the chromosomal location.[10] Dideoxy sequencing of *Pla2g6* was performed on an ABI 3100 Genetic Analyzer (Applied Biosystems Japan, Tokyo, Japan).

Behavioral Analysis

The hanging grip test was performed by placing a mouse on a plastic plate with round holes (Ø 7 mm with a 9-mm pitch) and then turning the plate upside down at a height of ~20 cm above the cage floor. The time that elapsed until the animal fell was recorded three times and the cutoff time was set at 30 seconds. Footprint patterns were obtained by painting the hindpaws with ink.

Histochemical Analysis

Mice were anesthetized with a lethal dose of pentobarbital sodium and transcardially perfused with 0.1 M phosphate buffer, pH 7.4, followed by 4% paraformaldehyde in 0.1 M phosphate buffer. Tissues including the brain and spinal cord were dissected and immersion-fixed in the same fixative overnight. After embedding in paraffin, 6-mm sections were prepared and stained with H&E. For electron microscopy, the animals were transcardially perfused with 0.1 M phosphate buffer, followed by 3% glutaraldehyde in 0.1 M phosphate buffer. Tissues were processed as described[11] and embedded in Epon 812 (Polysciences, Warrington, PA). Semithin sections were stained with toluidine blue for viewing under the light microscope. Ultrathin sections were stained with uranyl acetate and lead citrate and examined under a Hitachi H-7500 electron microscope.
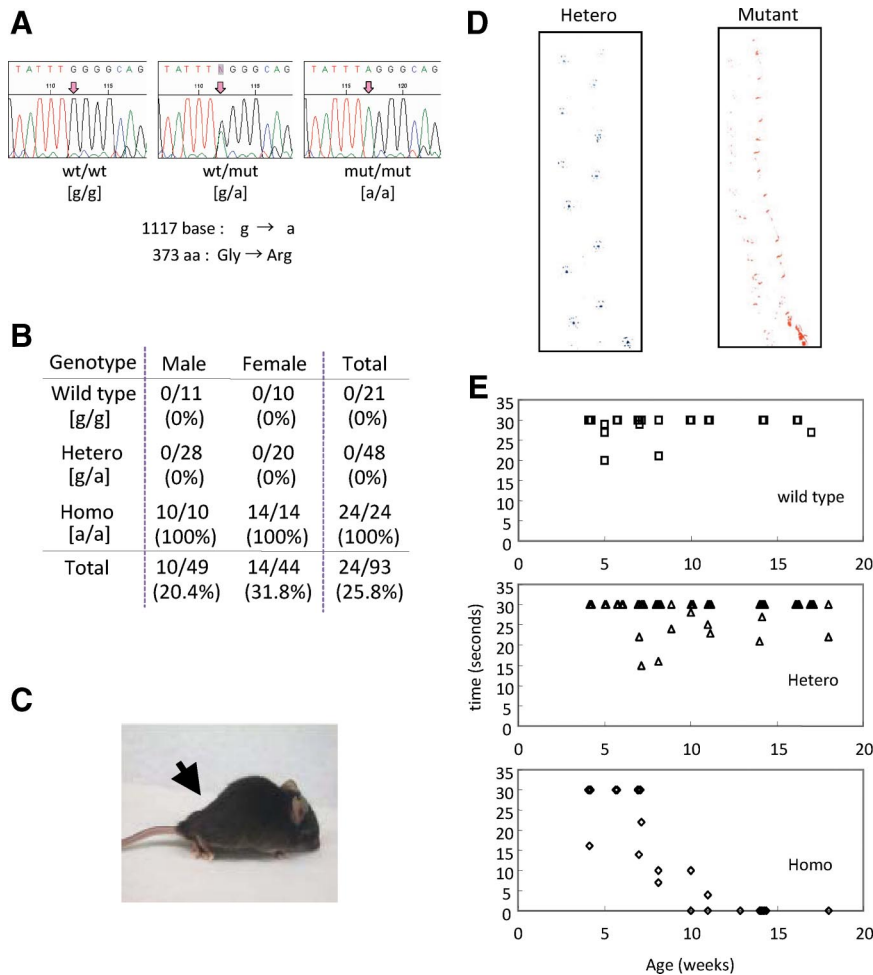
Figure 1. Mutation in the coding region of Pla2g6 induces motor dysfunction that begins at 7 to 8 weeks old. **A:** Sequencing of *Pla2g6* revealed a G to A transition leading to a nonconservative amino acid exchange at position 373 from glycine (G) to arginine (R). **B:** Heterozygotes were randomly mated, and 96 offspring were genotyped and observed. Numbers (and percentage) of mice that developed the motor dysfunction are indicated. **C:** Representative photograph of the *Pla2g6-inad* mutant at 12 weeks of age. The **arrow** represents muscle atrophy in the lower body. **D:** Representative footprint patterns of *Pla2g6-inad* heterozygotes and homozygotes at 15 weeks of age. **E:** Results of hanging grip test. Wild-type ($n = 25$), heterozygote ($n = 66$), and homozygote mice ($n = 26$) were tested as described in the *Materials and Methods*. The mean time for two trials was plotted against age.

PCR, Western Blot Analysis, and Lipid-Catalyzing Activity

cDNA was prepared from brain samples with SuperScript III reverse transcriptase (Invitrogen, Carlsbad, CA), and real-time PCR was performed with an ABI 7300 system using commercially obtained primers (Applied Biosystems, Foster City, CA). Point and deletion mutations of Pla2g6 were generated using PCR-mediated site-directed mutagenesis. All *Pla2g6* sequences were confirmed by sequence analysis. Immunoblot analysis was performed as described previously[12] using a polyclonal anti-Pla2g6 antibody (Cayman Chemical, Ann Arbor, MI). Lipid-catalyzing activity was determined as described previously[13] using 0.02 μCi of L-α-dipalmitoyl[2-palmi-toyl-1-^{14}C]-phosphatidylcholine (Perkin-Elmer Life and Analytical Sciences, Waltham, MA).

Results

In the G3, we recognized that several mice (~6%) developed severe gait difficulty before 10 weeks of age. Our initial pathological test suggested the existence of neurodegenerative disease in these mice. Analysis of DNA pools from B6/C3H × B6/C3H hybrid mutants ($n = 51$) detected homozygosity for B6 DNA only in a 2.0-cM interval around the D15SNP25 marker (Supplemental Table S1, see *http://ajp.amjpathol.org*). This interval includes *Pla2g6*, which has been recently reported as the causative gene for human INAD. In fact, sequencing of *Pla2g6* in the mutant mice revealed a G to A transition at 1117 base (Figure 1A), leading to a nonconservative amino acid exchange from glycine (G) to arginine (R) at position 373 (Universal Protein Resource Database, http://www.uniprot.org/uniprot/P97819, for mouse Pla2g6). This mutation is localized in the ankyrin repeat of Pla2g6, the mutation (G to R at the ankyrin repeat) that was also identified in patients with INAD[3] (the patients developed early disease as did other patients with INAD; S. Hayflick, Oregon Health & Science University, personal communication). Therefore, we designated this mutant the *Pla2g6-inad* mouse. After the genotyping, heterozygotes of *Pla2g6-inad* were randomly mated, and 96 offspring were genotyped and observed. All of the homozygotes developed the motor dysfunction with a frequency of ~25% (Figure 1, B and C), in accordance with a recessive pattern of inheritance and Mendelian law. Heterozygote littermates showed no gross abnormality compared with wild-type mice even when observed over 18 months.

Within several weeks after birth, the *Pla2g6-inad* homozygotes displayed no apparent evidence of motor impairment but gradually developed abnormalities in gait

and movement. By the age of 7 to 8 weeks, all of the homozygotes started to display abnormal movement, particularly in their hindlimbs, which developed progressively thereafter. The footprint patterns of 12-week-old homozygotes indicate that they dragged their hindlimbs when walking and had an irregular stride, although heterozygotes showed normal gait (Figure 1D). When motor dysfunction was assessed by the hanging grip test, the homozygotes started to show the impairment by 7 weeks of age, and all of the homozygotes older than 10 weeks of age could not hold their body on the inverted plate (Figure 1E), whereas the heterozygotes and the wild-type mice showed no abnormality in this test. The motor impairment got more severe with aging, and all of the homozygotes became emaciated and died before 18 weeks of age. Older (~18-month-old) heterozygotes and wild-type littermates showed no difference in this test (not shown).

In pathological studies, the *Pla2g6-inad* homozygotes showed neurogenic group atrophy in their hindlimb muscles (Figure 2A), suggesting the existence of neurodegeneration. In fact, we found numerous spheroid formations throughout the central nervous system. When 16-week-old homozygotes were examined, the spheroids were prominently observed in gracile and cuneate nuclei of the brainstem as in human INAD[14] (Figure 2, B–D) but were also detected in cerebral cortex (not shown), thalamus (Figure 2F), substantia nigra (not shown), trigeminal motor nucleus (Figure 2G), cerebellar dentate nucleus (Figure 2, H and I), lumber spinal anterior horn (Figure 2, J and K), lumber corticospinal tract (Figure 2M), and lumber posterior funiculus (Figure 2, N and O). Electron microscopic investigation revealed that the spheroids contained tubulovesicular structures, vacuoles, vesicles, mitochondria, and amorphous matrix (Figure 2, C, D, I, K, and O), whereas the nerve cell bodies in the spheroid-containing region seemed intact (Figure 2, E and L). These structural features are remarkably similar to those reported in human INAD.[15] Young heterozygotes and wild-type littermates showed no abnormality in these pathological examinations. Even when 18-month-old heterozygotes and wild-type littermates were examined, only a few spheroid formations in gracile and cuneate nuclei were observed in both (data not shown), which seemed to be due to the normal aging process.

The precise mechanism of how the dysfunction of PLA2G6 leads to INAD phenotype has not been clarified. To gather the information for elucidating the mechanism, we performed molecular and biochemical analysis of mutated Pla2g6. Brain tissues from *Pla2g6-inad* homozygote expressed Pla2g6 mRNA and protein irrespective of their age, detected by RT-PCR and Western blotting, respectively, as heterozygotes and wild-type littermates (Figure 3, A and B). We then examined whether mutated Pla2g6 protein has enzyme activity catalyzing glycerophospholipid. Brain tissues were obtained and homogenized in a homogenate buffer including leupeptin, aprotinin, and phenylmethylsulfonyl fluoride, and the solution was subjected to the lipase assay. Unfortunately, we could not detect any differences between homozygotes, heterozygotes, and wild-type littermates in this analysis

(not shown), presumably because there are numerous other phospholipase activities in the homozygote samples. Therefore, we prepared recombinant Pla2g6 proteins and assessed their lipase activities (Figure 3C). The full-length but not the deletion mutant, which lacks the lipase domain of Pla2g6 (Pla2g6 Δ463–467) showed significant catalyzing activity (Figure 3D). Mutated Pla2g6, whose 1117 base has been transitioned from G to A, causing G373R amino acid exchange, showed no enzyme activity (Figure 3D). These results strongly suggest that Pla2g6 protein exists in the homozygote but its catalytic activity is lost.

Discussion

Subsequent to the clinical reports indicating that PLA2G6 is the causative gene for human INAD,[3,4] two independent research groups reported that the iPLA$_2\beta$-null mutant (iPLA$_2\beta$ knockout [KO]) mice develop a neurodegenerative phenotype resembling that of INAD.[16,17] Pathological examination showed spheroid formation throughout the nervous system. Therefore, *Pla2g6*-lacking and -mutated mice are primarily similar in terms of the completed phenotype. However, disease onset in iPLA$_2\beta$ KO mice is critically late: the KO mice did not exhibit major neurological abnormality by the age of 1 year. After this period, the KO mice gradually develop the neurological abnormality, including motor dysfunction and spheroid formation. These results provided the evidence that loss of iPLA$_2\beta$ protein causes the neuroaxonal degeneration, although the time course of the disease is different from that of human INAD. In this regard, the *Pla2g6-inad* mutant we reported in this study seems to closely reflect human INAD, as the gene defect is point mutation, which is detected in the ankyrin repeat, and disease onset occurs in an early stage in the life span. Our *Pla2g6-inad* mutant would be useful for further studies of pathogenesis and experimental interventions including screening for drugs preventing neurodegenerative diseases.

The reason that the point mutation in Pla2g6 resulted in earlier disease onset than the null mutation has not been clarified, although similar cases are known for other genes, eg, SOD1 for familial amyotrophic lateral sclerosis.[18] Besides the lipase activity, Pla2g6 is known to interact with other molecules and contribute to signal transduction.[2] Because mutated Pla2g6 protein existed in the homozygote, it may play a dominant-negative role, by which some intracellular signaling important for cellular homeostasis may be strongly inhibited and neurodegeneration was accelerated. Another possible explanation is that the G373R mutation may disrupt an alternatively spliced shorter isoform of Pla2g6, as the gene has been reported to undergo extensive alternative splicing generating multiple isoforms, which substantially modulate the PLA2 activity.[19]
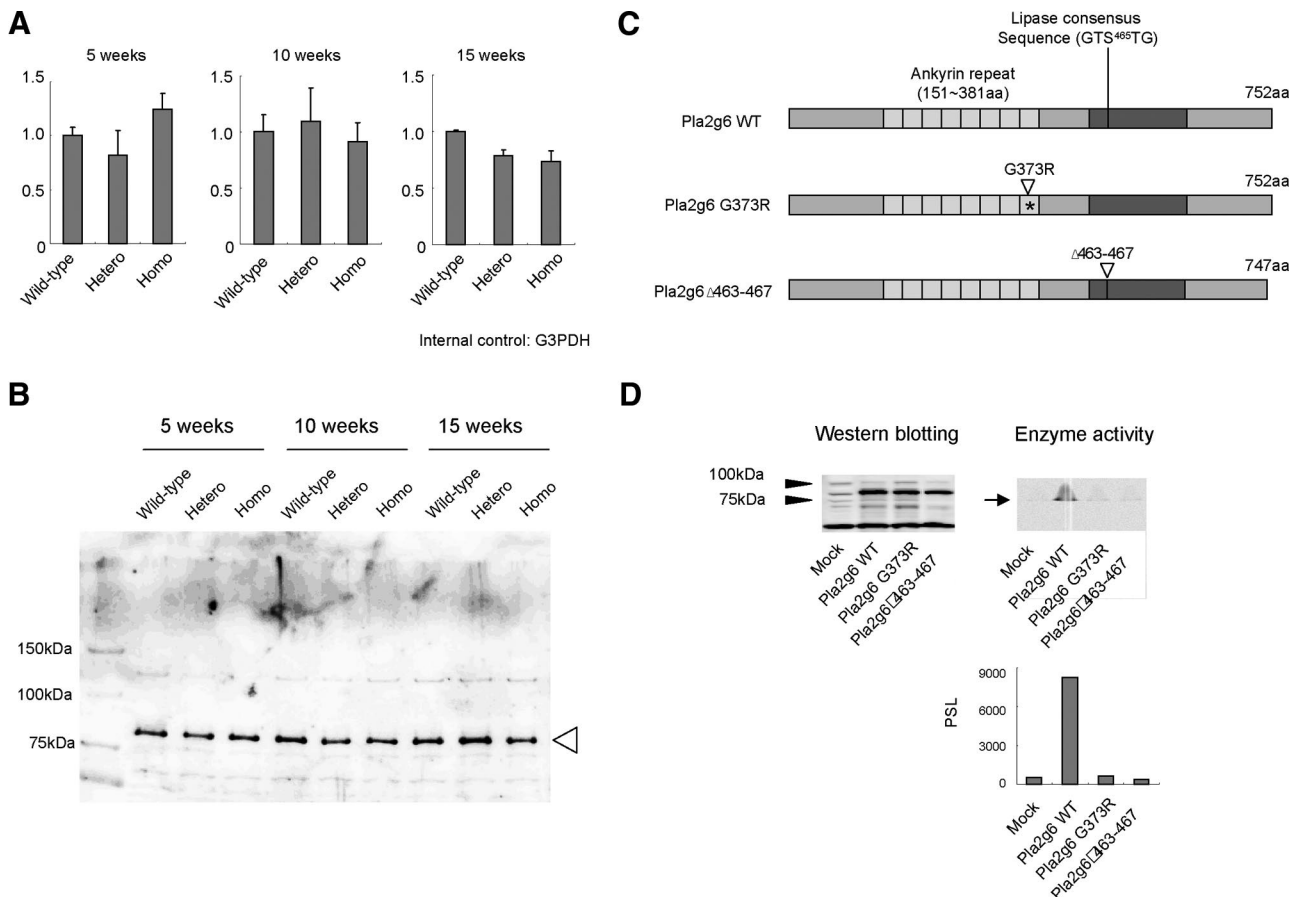
In this study, we could not formally exclude the possibility that there is an additional mutation in a neighboring gene of *Pla2g6*. According to the initial chromosomal mapping (Supplemental Table S1, see *http://ajp.amjpathol.org*) and the results of mating of 93 heterozygotes (Figure 1B),
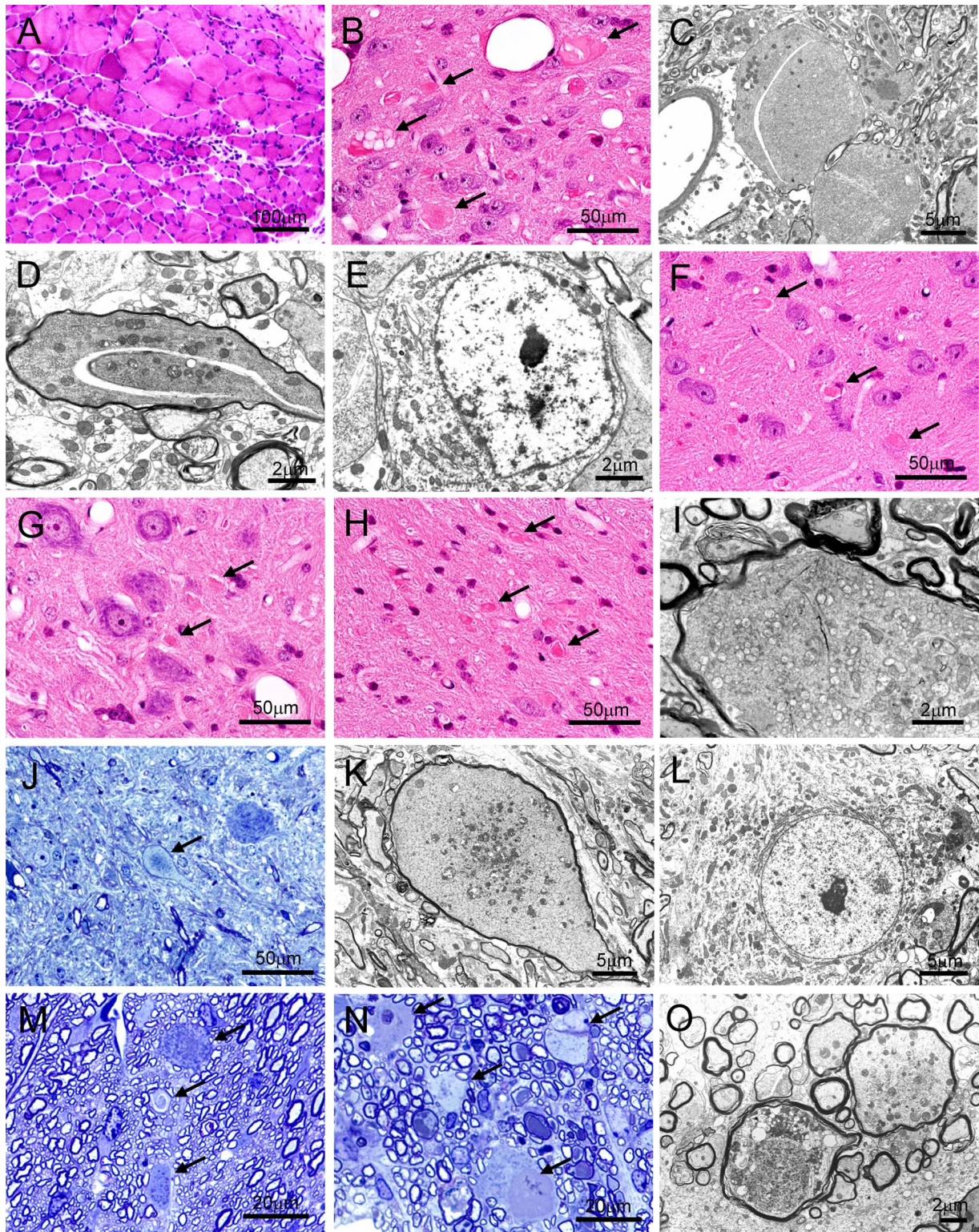
Figure 2. Neuropathological changes in the 16-week-old *Pla2g6-inad* mice. Photomicrographs of femoral muscle (**A**), gracile nucleus (**B–E**), thalamus (**F**), trigeminal motor nucleus (**G**), cerebellar dentate nucleus (**H** and **I**), lumber spinal anterior horn (**J–L**), lumber corticospinal tract (**M**), and lumber posterior funiculus (**N** and **O**). H&E (**A, B, F, G,** and **H**)- and toluidine blue (**J, M,** and **N**)-stained light micrographs and electron micrographs (**C, D, E, I, K, L,** and **O**). **Arrows** indicate spheroid formation. Electron microscopically, spheroids contain tubulovesicular structures, vacuoles, vesicles, mitochondria, and amorphous matrix (**C, D, I, K,** and **O**). The nerve cell bodies in gracile nucleus (**E**) and spinal anterior horn (**L**) appear normal. Representative data from three experiments.

A

5 weeks

10 weeks

15 weeks

Internal control: G3PDH

C

Lipase consensus
Sequence (GTS^{465}TG)

Ankyrin repeat
(151~381aa)

752aa

Pla2g6 WT

G373R

752aa

Pla2g6 G373R

*

Δ463–467

747aa

Pla2g6 Δ463–467

B

5 weeks   10 weeks   15 weeks

Wild-type Hetero Homo   Wild-type Hetero Homo   Wild-type Hetero Homo

150kDa

100kDa

75kDa

D

Western blotting   Enzyme activity

100kDa
75kDa

Mock Pla2g6 WT Pla2g6 G373R Pla2g6Δ463-467

Mock Pla2g6 WT Pla2g6 G373R Pla2g6Δ463-467

PSL

9000

6000

3000

Mock Pla2g6 WT Pla2g6 G373R Pla2g6Δ463-467

Figure 3. Expression and function of Pla2g6 in the *Pla2g6-inad* mutant. **A:** *Pla2g6* mRNA expression. Brain samples (two or more in each group) were obtained at the indicated age, and pooled cDNA samples were subjected to the real-time PCR analysis. glyceraldehyde-3-phosphate dehydrogenase (G3PDH) was used for the internal control. The relative values (mean ± SD of three wells) to the mean value of wild-type were indicated. There is no significant difference. **B:** Pla2g6 protein expression. Brain samples were obtained as in **A,** protein fractions were prepared, and pooled samples were subjected to the Western blotting analysis using anti-Pla2g6 antibody. Eighty-kilodalton bands represent Pla2g6 (**arrowhead**). Representative data from three experiments. **C:** Scheme of recombinant proteins. Pla2g6 WT is a wild-type Pla2g6, Pla2g6 G373R has a point mutation at 1117 base from g to a (**asterisk**), and Pla2g6 Δ463–467 lacks the lipase consensus sequence. **D:** Lipid catalyzing activity. Expression vectors (pcDNA3) encoding the recombinant Pla2g6s were transfected into HEK293 cells. After confirming the protein expression as in Figure 2 (**upper left**), lipid-catalyzing activity of each protein was examined using radio-labeled L-α-dipalmitoyl[2-palmitoyl-1-^{14}C]-phosphatidylcholine (**upper right**, **arrow** represents the catalyzed lipid). **Lower panel:** the lipid-catalyzing activities were graphed, PSL, photo-stimulated luminescence. Representative data from two independent experiments.

the range of the affected region was estimated to be less than 1.5 cM and contain ~38 genes (Genes & Markers Query, Mouse Genome Informatics, The Jackson Laboratory, Bar Harbor, ME). Subsequently, we have obtained at least 175 homozygotes and observed complete coincidence of the genotype and phenotype (data not shown), data that further narrowed down the region. On the other hand, neighboring this region in chromosome 15 are *N*-acetylglucosaminidase and arylsulfatase, which have been reported to be highly related with the development of neurodegeneration.[20,21] We have sequenced these genes in the *Pla2g6-inad* mice but failed to find any mutation (data not shown). Given this information, the possibility of the second mutation seems to weaken. However, further genetic investigation will be needed to precisely resolve this issue.

In the iPLA$_2\beta$ KO mice, an acceleration in age-related changes in bone morphology is observed, which became apparent at 6 months of age.[22] We also detected similar changes in the bone morphology in *Pla2g6-inad* mutant. At least 12-week-old or older mutants showed decreases

in both cortical and trabecular bone volume (Supplemental Figure S1, see *http://ajp.amjpathol.org*). Therefore, various phenotypes observed in iPLA$_2\beta$ KO mice such as insulin secretion deficiency[23] or insufficient spermatogonia[24] may also be expressed in the *Pla2g6-inad* mutant with early onset. Thus, use of the *Pla2g6-inad* mutant may accelerate research regarding iPLA$_2\beta$. Furthermore, we found that *Pla2g6-inad* mutants have severe thymic atrophy because of an almost complete loss of CD4CD8 double-positive thymocytes (Supplemental Figure S2, see *http://ajp.amjpathol.org*). Therefore, critical further investigation of the *Pla2g6-inad* mutant may contribute to elucidating a novel disease phenotype in INAD and also etiology of the intractable neurodegenerative disease.

University), and Yoshinori Arai (Nihon University School of Dentistry) for valuable discussions regarding this study.

References

1. Burke JE, Dennis EA: Phospholipase A2 structure/function, mechanism and signaling, J Lipid Res 2009, 50(Suppl):S237–S242

2. Ma Z, Turk J: The molecular biology of the group VIA Ca^{2+}-independent phospholipase A2. Prog Nucleic Acid Res Mol Biol 2001, 67:1–33

3. Morgan NV, Westaway SK, Morton JE, Gregory A, Gissen P, Sonek S, Cangul H, Coryell J, Canham N, Nardocci N, Zorzi G, Pasha S, Rodriguez D, Desguerre I, Mubaidin A, Bertini E, Trembath RC, Simonati A, Schanen C, Johnson CA, Levinson B, Woods CG, Wilmot B, Kramer P, Gitschier J, Maher ER, Hayflick SJ: PLA2G6, encoding a phospholipase A2, is mutated in neurodegenerative disorders with high brain iron. Nat Genet 2006, 38:752–754

4. Khateeb S, Flusser H, Ofir R, Shelef I, Narkis G, Vardi G, Shorer Z, Levy R, Galil A, Elbedour K, Birk OS: PLA2G6 mutation underlies infantile neuroaxonal dystrophy. Am J Hum Genet 2006, 79:942–948

5. Nardocci N, Zorzi G, Farina L, Binelli S, Scaioli W, Ciano C, Verga L, Angelini L, Savoiardo M, Bugiani O: Infantile neuroaxonal dystrophy: clinical spectrum and diagnostic criteria. Neurology 1999, 52:1472–1478

6. Seitelberger F: The Hallervorden-Spatz disease. Nervenarzt 1966, 37:482–493

7. Ramaekers VT, Lake BD, Harding B, Boyd S, Harden A, Brett EM, Wilson J: Diagnostic difficulties in infantile neuroaxonal dystrophy: a clinicopathological study of eight cases. Neuropediatrics 1987, 18:170–175

8. Cook MC, Vinuesa CG, Goodnow CC: ENU-mutagenesis: insight into immune function and pathology. Curr Opin Immunol 2006, 18:627–633

9. Masuya H, Nakai Y, Motegi H, Niinaya N, Kida Y, Kaneko Y, Aritake H, Suzuki N, Ishii J, Koorikawa K, Suzuki T, Inoue M, Kobayashi K, Toki H, Wada Y, Kaneda H, Ishijima J, Takahashi KR, Minowa O, Noda T, Wakana S, Gondo Y, Shiroishi T: Development and implementation of a database system to manage a large-scale mouse ENU-mutagenesis program. Mamm Genome 2004, 15:404–411

10. Inoue M, Sakuraba Y, Motegi H, Kubota N, Toki H, Matsui J, Toyoda Y, Miwa I, Terauchi Y, Kadowaki T, Shigeyama Y, Kasuga M, Adachi T, Fujimoto N, Matsumoto R, Tsuchihashi K, Kagami T, Inoue A, Kaneda H, Ishijima J, Masuya H, Suzuki T, Wakana S, Gondo Y, Minowa O, Shiroishi T, Noda T: A series of maturity onset diabetes of the young, type 2 (MODY2) mouse models generated by a large-scale ENU mutagenesis program. Hum Mol Genet 2004, 13:1147–1157

11. Watabe K, Ida H, Uehara K, Oyanagi K, Sakamoto T, Tanaka J, Garver WS, Miyawaki S, Ohno K, Eto Y: Establishment and characterization of immortalized Schwann cells from murine model of Ni-

12. Wolf MJ, Gross RW: Expression, purification, and kinetic characterization of a recombinant 80-kDa intracellular calcium-independent phospholipase A$_2$. J Biol Chem 1996, 271:30879–30885

13. Seashols SJ, del Castillo Olivares A, Gil G, Barbour SE: Regulation of group VIA phospholipase A$_2$ expression by sterol availability. Biochim Biophys Acta 2004, 1684:29–37

14. Itoh K, Negishi H, Obayashi C, Hayashi Y, Hanioka K, Imai Y, Itoh H: Infantile neuroaxonal dystrophy—immunohistochemical and ultrastructural studies on the central and peripheral nervous systems in infantile neuroaxonal dystrophy. Kobe J Med Sci 1993, 39:133–146

15. Yagishita S, Kimura S: Infantile neuroaxonal dystrophy: histological and electron microscopical study of two cases. Acta Neuropathol 1974, 29:115–126

16. Malik I, Turk J, Mancuso DJ, Montier L, Wohltmann M, Wozniak DF, Schmidt RE, Gross RW, Kotzbauer PT: Disrupted membrane homeostasis and accumulation of ubiquitinated proteins in a mouse model of infantile neuroaxonal dystrophy caused by PLA2G6 mutations. Am J Pathol 2008, 172:406–416

17. Shinzawa K, Sumi H, Ikawa M, Matsuoka Y, Okabe M, Sakoda S, Tsujimoto Y: Neuroaxonal dystrophy caused by group VIA phospholipase A2 deficiency in mice: a model of human neurodegenerative disease. J Neurosci 2008, 28:2212–2220

18. Rothstein JD: Current hypotheses for the underlying biology of amyotrophic lateral sclerosis, Ann Neurol 2009, 65(Suppl 1):S3–S9

19. Larsson PK, Claesson HE, Kennedy BP: Multiple splice variants of the human calcium-independent phospholipase A2 and their effect on enzyme activity. J Biol Chem 1998, 273:207–214

20. Gieselmann V, Matzner U, Hess B, Lullmann-Rauch R, Coenen R, Hartmann D, D'Hooge R, DeDeyn P, Nagels G: Metachromatic leukodystrophy: molecular genetics and an animal model. J Inherit Metab Dis 1998, 21:564–574

21. Yogalingam G, Hopwood JJ: Molecular genetics of mucopolysaccharidosis type IIIA and IIIB: diagnostic, clinical, and biological implications. Hum Mutat 2001, 18:264–281

22. Ramanadham S, Yarasheski KE, Silva MJ, Wohltmann M, Novack DV, Christiansen B, Tu X, Zhang S, Lei X, Turk J: Age-related changes in bone morphology are accelerated in group VIA phospholipase A$_2$ (iPLA2β)-null mice. Am J Pathol 2008, 172:868–881

23. Bao S, Song H, Wohltmann M, Ramanadham S, Jin W, Bohrer A, Turk J: Insulin secretory responses and phospholipid composition of pancreatic islets from mice that do not express group VIA phospholipase A$_2$ and effects of metabolic stress on glucose homeostasis. J Biol Chem 2006, 281:20958–20973

24. Bao S, Miller DJ, Ma Z, Wohltmann M, Eng G, Ramanadham S, Moley K, Turk J: Male mice that do not express group VIA phospholipase A$_2$ produce spermatozoa with impaired motility and have greatly reduced fertility. J Biol Chem 2004, 279:38194–38200

emann-Pick disease type C (spm/spm). J Peripher Nerv Syst 2001, 6:85–94